NUCLEAR SCIENCE AND TECHNIQUES **25**, 060201 (2014)

Pulsed intense electron beam emittance measurement

ZHANG Zhuo (张卓)[1,*] and JIANG Xiao-Guo (江孝国)[1]

[1]*Institute of Fluid Physics, China Academy of Engineering Physics, Mianyang 621900, China*

(Received January 22, 2014; accepted in revised form May 19, 2014; published online December 15, 2014)

Recently we measured with the Modified Three Gradient Method (MTGM) the beam emittance of an injector constructed in 2012, which was designed to provide a 2.4 kA, 2.6 MeV electron beam. The MTGM is a non-intercept indirect method, which is based on the three gradient type measurements of beam profiles and subsequent data processing which helps to get the least square solution to the beam emittance. Beam profiles under different currents of guiding coil are measured using Cerenkov radiation given off by a piece of quartz glass in the beam tube, which is recorded with a CCD camera. MTGM Code is developed to realize the data fitting as well as beam transport simulation, in which both the σ matrix method and the numerical solution of root-mean-square beam envelope equation are used. The error is also analyzed.

Keywords: Emittance measurements, High current beam, Modified three gradient method

DOI: 10.13538/j.1001-8042/nst.25.060201

I. INTRODUCTION

In most applications, emittance and brightness are the main figures of merit of particle beams. The horizontal emittance and vertical emittance are related to the beam brightness, which is defined as $B = I/\pi^2\varepsilon_x\varepsilon_y$. Here, the horizontal (vertical) emittance is usually defined by considering the x and x' phase space, as the area (optionally divided by π) of the ellipse containing 95% (or an arbitrary number) of all particles in its interior. Low beam emittance is key to achieving the required spot size at the output focus of the beam line.

The Liouville theorem [1] states that volumes in phase space are invariant for a Hamiltonian system. In linear accelerators, where the particle energy is varied, the emittance is not invariant. Instead, one defines the so-called normalized emittance, $\varepsilon_n = \beta\gamma\varepsilon$. The normalized emittance is conserved during acceleration.

Conventional measurements of emittance include the pepper pot method [2], the three gradient method [3], the MTGM [4, 5], etc. Here we use the MTGM for its advantages, such as the online feasibility for non-destructive procedure.

The main concept of MTGM is shown in Fig. 1. It is based on the three gradient type measurements of the beam radius and a data fitting to the measured cross-over curve.

Under a certain current of guiding coil, supposing that ε and initial conditions (R_0, R_0') are known, the root-mean-square beam envelope of an axially symmetric beam is described by the following equation [6]

$$R''_{\rm rms} + k^2 R_{\rm rms} - \frac{K}{2R_{\rm rms}} - \frac{\varepsilon^2_{\rm rms}}{R^3_{\rm rms}} = 0, \qquad (1)$$

$$k = \frac{ecB_z}{2\beta\gamma m_0 c^2}, \quad K = \frac{2I_b}{17045\beta^3\gamma^3}, \qquad (2)$$

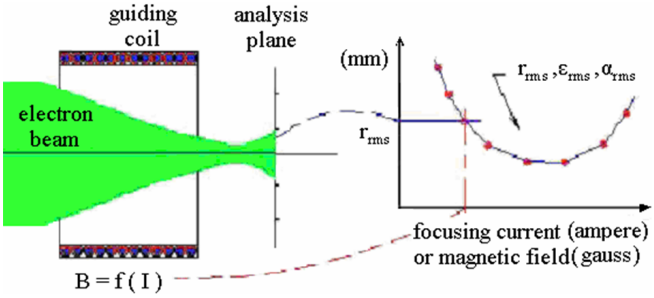

Fig. 1. (Color online) Diagram of MTGM. The beam profile sizes at analysis plane change corresponding to focusing current in guiding coil. Multi measurements provide a set of scattered data (red dots). Fit to this data set with a cross-over curve (blue line) solved from beam envelope equation, we can get a least square solution of beam emmitance.

where $R_{\rm rms}$ is the beam radius and $\varepsilon_{\rm rms}$ is the beam emittance normalized to the beam energy. It is found that $\varepsilon_{\rm rms}$ remains a constant during non-accelerating transport procession. The foot rms denotes root-mean-square, which will be dropped for the remainder of this paper for the sake of concession. Note that all ε in the following is edge emittance normalized to energy. k is one half the cyclotron wave numbers with B_z, the axial magnetic field determined by focusing the current of the guiding coil. K is the general diversion coefficient with $I_{\rm b}$, the beam current, measured by the CVRs. β and γ are relativistic factors and can be calculated from beam energy, which is measured with a capacitive probe mounted in the gap between the accelerator cells.

Equation 1 can be solved with the numerical method by converting the problem to a 1-order differential equation group, which can be solved with the Runge-Kutta method [7]. Solving the equation under a different magnetic field will generate a set of beam radii data, from which a cross-over curve revealing the relation between beam radius at the analysis plane with magnetic field can be constructed. Reversely, if we can get the cross-over curve through experiments, (ε, R_0, R_0') can be deduced by the data fitting method. In our

* Corresponding author, zhangzhuo96@tsinghua.org.cn

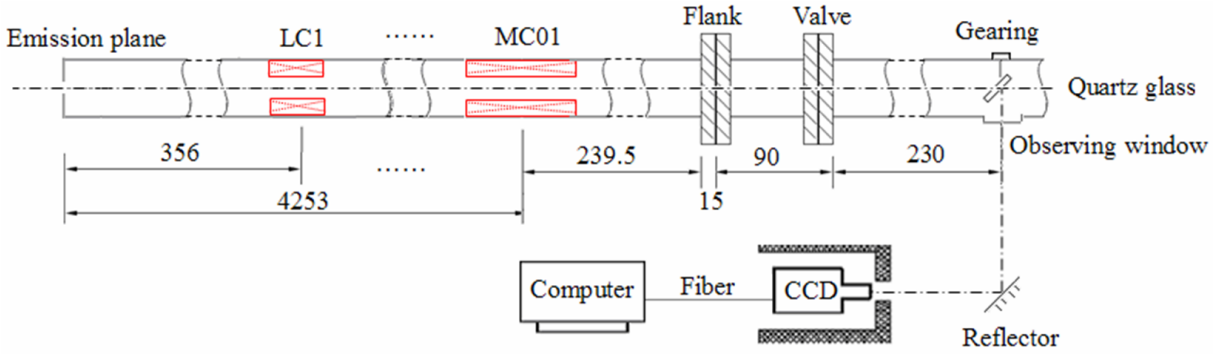

Fig. 2. (Color online) Sketch of experimental setup. Beam from emission plane transports through a set of coils and interacts with a quartz glass at the back of the analysis plane which visible light is given out and accepted by a CCD camera. The information of beam profile size is later detached by a computer software.

work, the σ matrix method is used as an aid to find the least square fitting to the cross-over curve.

II. MEASUREMENTS

Beam profiles are measured by making use of Cerenkov Radiation (CR) [8], which is given off by charged particles traversing a transparent dielectric medium in which its velocity exceeds that of light. It is preferred in experiments profiting from its definite direction, rapid response time, and the proportional property of the yield of photons to the number of electrons. Given off at the analysis plane, which is located at a distance of 574.5 mm downstream from the center of the guiding coil, the CR light is reflected by a reflector and accepted by a CCD camera. Through a fiber, it is transmitted on to an online computer. The experimental sketch is shown in Fig. 2.

The parameters of the solenoid coils on the experimental beam line are listed in Table 1.

TABLE 1. Solenoid Coils Parameter

Solenoid No.	Length (m)	R_O (m)	R_I (m)	Excitation (A×n)	Position (m)
LC1	0.172	0.186	0.164	31476	0.356
LC2	0.217	0.186	0.164	0	0.774
IC01	0.373	0.248	0.230	10560	1.386
IC02	0.373	0.248	0.230	13200	1.859
IC03	0.373	0.248	0.230	17160	2.332
IC04	0.373	0.248	0.230	15840	2.805
IC05	0.373	0.248	0.230	17160	3.278
VC	0.373	0.248	0.230	31680	3.740
MC01	0.338	0.121	0.093	0-61440	4.253

The images of beam profiles under different focusing currents are shown in Fig. 3.

Scan the images in the radial direction and draw its gray scale curve, from which the beam radii are read out (see Table 3 in Section III).

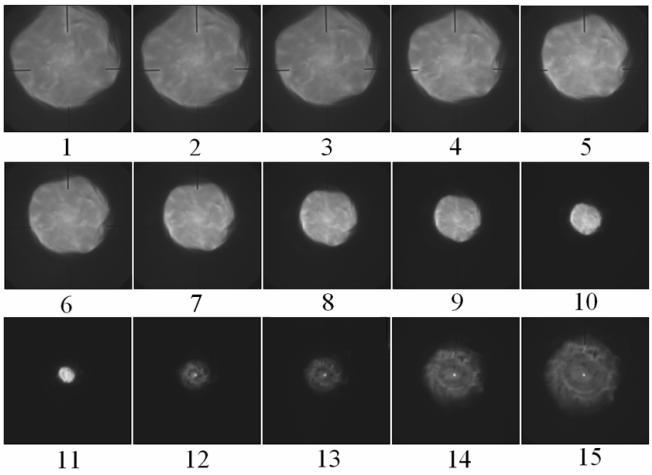

Fig. 3. Measurements of beam profiles. Beam profiles change while adjusting focusing current of MC01. At 11Ampere, beam profile reaches its minimum.

III. SIMULATION RESULTS AND DISCUSSION

MTGM was applied to measure the emittance of a space charge dominated electron beam and has been tested to be effective.

The magnetic field under different current supply is calculated. Fig. 4 plots the magnetic field curve from $z_0 = 3$ m to $z_0 = 4.642$ m. The plot reveals the proportional property of the magnetic field to the current supply.

The start point of calculation is selected to be $z = 3$ m, a position where the magnetic field of MC01 is trivial and the initial conditions are relatively constant during different measurements times.

MTGM CODE is designed to aid in searching for (ε, R_0, R_0') by fitting the least square to the measured (R_i, I_i).

The Beam envelope equation is a second order derivative function with a varying coefficient, whose explicit solution is difficult to get by integration directly [9]. However, the σ matrix method provides a concise way to find the direct relation between R and initial conditions. It makes it possible

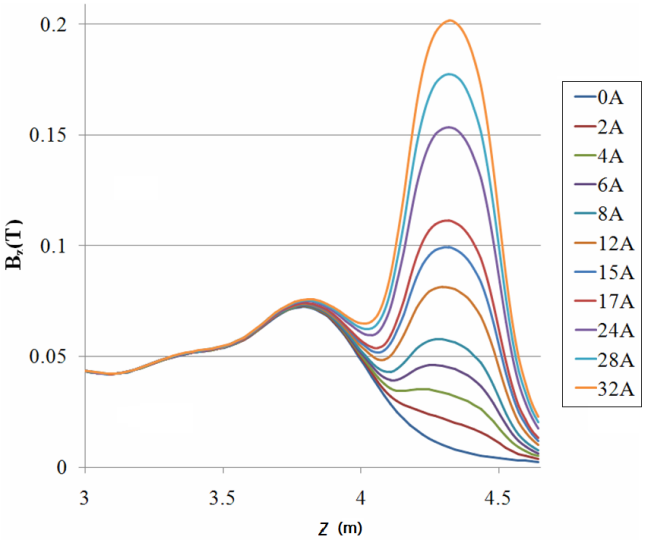

Fig. 4. (Color online) Transport magnetic field. The magnetic field is constant at $z = 3$ m while changing focusing current of MC01 at $z = 4.253$ m.

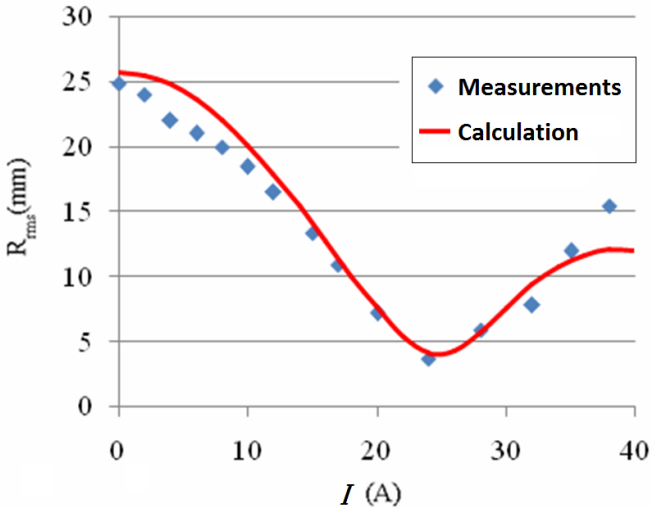

Fig. 5. (Color online) R–I data and fitting cross-over curve. Measurements (blue diamonds) are the rms radius of beam at different focusing currents. Calculation (red curve) is the best fit calculated from the beam envelope equation.

to use the data fitting least square method [10]. As a matter of fact, the σ matrix method is a beam transport solving method which can have an independent effect even though it plays the role of a complement to the beam envelope method in this way. After a great deal of manipulation, we obtained

$$R = \sqrt{M_{11}^2 R_0^2 + 2M_{11}M_{12}\left(\pm\sqrt{R_0^2\widetilde{R_0'}^2 - \varepsilon^2}\right) + M_{12}^2\widetilde{R_0'}^2}, \tag{3}$$

here, M is the transport matrix of the beam line as a whole [11]. Special attention should be paid to the $\widetilde{R_0'}$ associated with the σ matrix in this function, since it is not the derivative of R over z, but the beam angular envelope, which is the maximum of r_0' in the phase space [12] and can be calculated by solving the ellipse function in phase space. As a matter of fact, the $(\varepsilon, R_0, \widetilde{R_0'})$ here is a set of initial conditions of the σ matrix method, which is equivalent to the (ε, R_0, R_0') of the beam envelope equation. Both sets can be derived from one another by taking the derivative over z of Eq. (3) at $z = z_0$. The sign of the second term is determined by the direction of the ellipse in phase space, negative for converging procession, while positive for diverging procession.

The least square method demands the minimum of

$$\|\delta\|_2^2 = \sum_{i=1}^{m}\left[R(i_i) - R_i\right]^2 = \min_{R_0,R_0',\varepsilon}\sum_{i=1}^{m}\left[R(i_i) - R_i\right]^2. \tag{4}$$

This requires the zero derivatives of $\|\delta\|_2^2$ to ε, R_0, R_0':

$$\frac{\partial\|\delta\|_2^2}{\partial\varepsilon} = 0, \quad \frac{\partial\|\delta\|_2^2}{\partial R_0} = 0, \quad \frac{\partial\|\delta\|_2^2}{\partial R_0'} = 0. \tag{5}$$

A three dimension equations set on R_0, R_0', ε can be obtained by substituting the expression of R and $\|\delta\|_2^2$ into the functions above. By solving the equation set, we can get the solution of R_0^*, $R_0'^*$, ε^* proscribing by the least square approximation to the measured data.

TABLE 2. The least square solution of (ε, R_0, R_0')

Parameters	ε^* (π · mm · mrad)	R_0^* (mm)	$R_0'^*$ (mrad)
Values	1120	9	18

The emittance and the corresponding initial conditions (ε^*, R_0^*, $R_0'^*$) are listed in Table 2.

Using the (ε^*, R_0^*, $R_0'^*$) above, the numerical solution of the beam envelope equation is obtained with the forth order Runge-Kutta method.

The measured R–I data and calculated data is listed in Table 3.

TABLE 3. Radii versus focusing current

NO.	I (A)	R_i (mm)	$R(I_i)$ (mm)	δ_i (mm)
1	0	24.9	25.73	0.83
2	2	24.0	25.49	1.49
3	4	22.0	24.79	2.79
4	6	21.0	23.65	2.65
5	8	19.9	22.08	2.18
6	10	18.4	20.14	1.74
7	12	16.5	17.86	1.36
8	15	13.4	14.08	0.68
9	17	10.9	11.41	0.51
10	20	7.2	7.56	0.36
11	24	3.7	4.13	0.43
12	28	5.9	5.75	−0.15
13	32	7.8	9.39	1.59
14	35	12.0	11.32	−0.68
15	38	15.5	12.09	−3.41

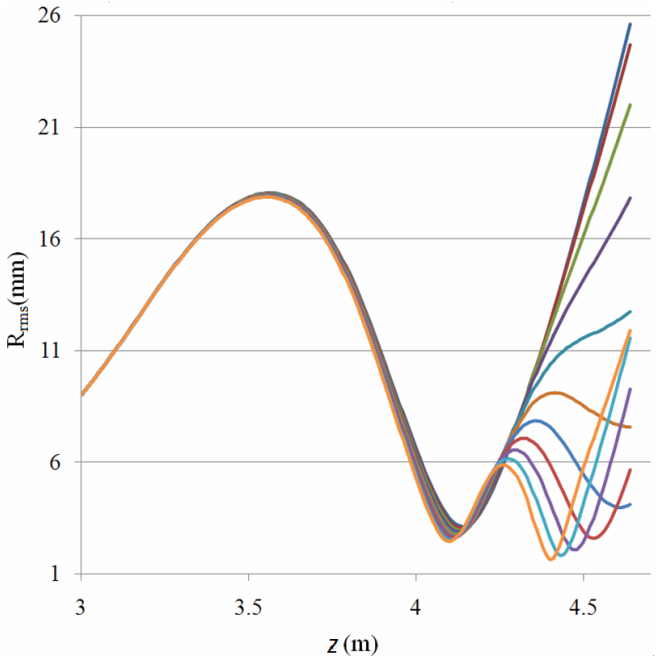

Fig. 6. (Color online) Beam Envelopes(Lines are the same as Fig. 4). Beam envelopes are sharply modulated by focusing current of MC01. The minimum should be near the blue one, within the range between the blue one and the red one.

The cross-over curve corresponding to (ε^*, R_0^*, $R_0'^*$) is plotted in Fig. 5.

The beam envelopes are shown in Fig. 6.

Precision of the method requires sufficient data acquisition within a wide range. This can be realized by carefully choosing of the distance between the center of guiding coil and the analysis plane, as well as their position within the beam envelope evolution.

Now let's write equation (1) in the following form

$$R''_{\rm rms} = -k^2 R_{\rm rms} + \frac{K}{2R_{\rm rms}} + \frac{\varepsilon^2_{\rm rms}}{R^3_{\rm rms}}, \tag{6}$$

here, the term on the left is a kind of force on the beam envelope, while the terms on the right side of the equation represent contributions of different forces, including the focusing force of the axial magnetic field B_z and defocusing forces from the space charge effect and beam emittance.

This will be clearer if we deal with the three functions individually. The focusing effect of the axial magnetic field over a small step can be described by

$$R = \frac{\sqrt{(kR_0)^2 + R_0'^2}}{kR_0} \sin\left[k(z-z_0) + \arctan\left(-k\frac{R_0}{R_0'}\right)\right]. \tag{7}$$

The effective emittance force describes the beam transport in drift space.

$$R = \sqrt{\left[\frac{(R_0R_0')^2+\varepsilon^2}{R_0^2}\right]\left[z - z_0 + \frac{R_0^3R_0'}{(R_0R_0')^2+\varepsilon^2}\right]^2 + \frac{\varepsilon^2R_0^2}{(R_0R_0')^2+\varepsilon^2}}. \tag{8}$$

This equation defines a hyperbolic evolution of the beam envelope under the effect of emittance, restricted by which the minimum of beam radius is

$$R_{e,\min} = \frac{\varepsilon R_0}{\sqrt{(R_0R_0')^2+\varepsilon^2}}. \tag{9}$$

The effect of space charge can not be expressed explicitly. However, through integrating the equation over a small step, we can get

$$R' = \pm\sqrt{R_0' + K\ln\frac{R}{R_0}}. \tag{10}$$

or written in the form

$$R = R_0 e^{-\frac{R'^2 - R_0'^2}{K}}. \tag{11}$$

This equation representing the expanding effect of space charge force restricted by the minimum of beam radius is

$$R_{\rm sc,min} = R_0 e^{-\frac{R_0'^2}{K}}. \tag{12}$$

When R is a big number, or at positions far away from the bottom of the cross over curve, where the magnetic field focusing force dominates, R is sensitive to variation in magnetic field. However, the situation changed at the bottom of the cross over curve, where R is a small number and is mainly determined by emittance and space charge force.

Therefore, finding the exact minimum spot of the crossover curve is crucial to determining the beam emittance. A feasible measure is to get as much data as possible in the vicinity of the bottom of the cross-over curve by shortening the steps of the guiding current. Repeated measurements at the same guiding current also help to eliminate the intrinsic uncertainty of beam size.

The error is mainly introduced by: (1) error of beam radius measurements; (2) error of beam energy and beam current; (3) error of the MTGMCODE. Elaborate error analysis has been done elsewhere [13]. It is found that the influence of (1) affects the precision while (2) and (3) are relatively trivial.

We simulated the transport of beams with different emittances, increasing from 120 to 1720 in an arithmetical progression, as shown in Fig. 7. Each step between two adjacent curves is 20 0π mm mrad.

By taking partial derivatives of Eq. (3) over ε, R_0, $\tilde{R}_0'$, we

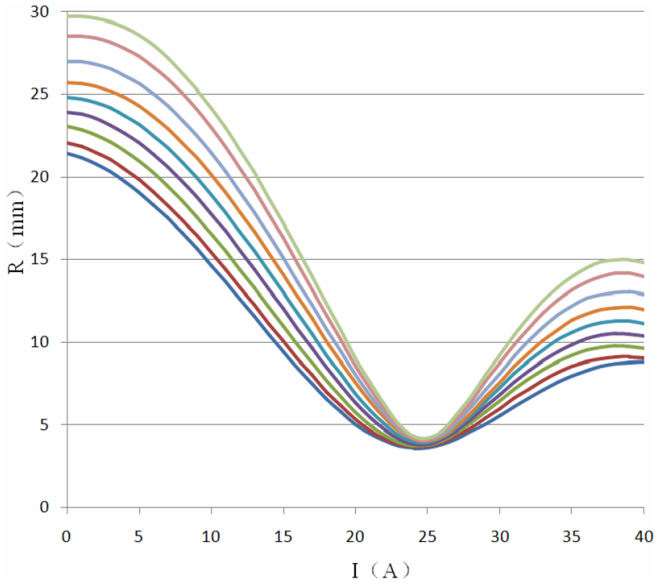

Fig. 7. (Color online) A set of cross-over curves and corresponding emittance. Different radius levels give different emittances.

TABLE 4. Corresponding Parameters

NO.	ε (π mm mrad)	R_0 (mm)	R_0' (mm)
1	120	13.9	2.2
2	320	13.8	4.5
3	520	13.2	8.2
4	720	11.9	12.3
5	920	10.5	15.5
6	1120	9	18
7	1320	7.8	19.6
8	1520	6.6	20.2
9	1720	5.8	18.5

can get the error formula

$$\begin{aligned}\Delta R =& \frac{\partial R}{\partial \varepsilon}\Delta\varepsilon + \frac{\partial R}{\partial R_0}\Delta R_0 + \frac{\partial R}{\partial R_0'}\Delta \tilde{R}_0' \\ =& \mp \frac{\varepsilon\Delta\varepsilon}{R}\cdot\frac{M_{11}M_{12}}{\sqrt{R_0^2R_0'^2-\varepsilon^2}} \\ &+ \frac{R_0\Delta R_0}{R}\left(M_{11}^2 \pm \frac{M_{11}M_{12}}{\sqrt{R_0^2R_0'^2-\varepsilon^2}}\cdot\tilde{R}_0'^2\right) \\ &+ \frac{\tilde{R}'\Delta\tilde{R}_0'}{R}\left(M_{12}^2 \pm \frac{M_{11}M_{12}}{\sqrt{R_0^2R_0'^2-\varepsilon^2}}\cdot R_0^2\right).\end{aligned} \tag{13}$$

Beam radius measurement uncertainty will result in errors in the discrimination of R_0, R_0', and ε. Substituting R_0, ε in the formula above with R_0^*, ε^*, and $\tilde{R}_0'$ calculated from R_0' by taking the derivative over z of Eq. (3) at $z = z_0$. For a given transport system, M_{11} and M_{12} are functions of z determined by its structure and parameters. The error formula can be written in the form

$$\Delta R = \alpha\frac{\varepsilon\Delta\varepsilon}{R} + \beta\frac{R_0\Delta R_0}{R} + \gamma\frac{\tilde{R}_0'\Delta\tilde{R}_0'}{R}, \tag{14}$$

here, R is the result of the least square fitting to the measured data. For each point on the plot in Fig. 7, the error of ε is roughly in positive proportion to that of R. The relation between emittance and radii can be roughly formulated as

$$\Delta\varepsilon(\pi\,\text{mm mrad}) = (200 \sim 1600)\Delta R(\text{mm}). \tag{15}$$

This means that around the minimum of the cross-over curve, small radius measurement uncertainty may result in large emittance calculation errors, about 8 times that of the measurements far away from it. For example, at the bottom of the cross over curve, a 1 mm radius measurement uncertainty will cause about a 160 0π mm mrad emittance calculation error, while at the upper side of the curve, the same radius measurement uncertainty will cause only about a 20 0π mm mrad emittance calculation error, only one eighth of the former.

The relative error is

$$\frac{\Delta\varepsilon}{\varepsilon} = \eta\frac{\Delta R}{R}. \tag{16}$$

Under measuring conditions, η is within the region of 6 and 10, with 10 at the lower part of the plot and 6 at the upper part.

The parameters corresponding to each plot are listed in Table 4, including the emittance, and the initial values of the radius and the spreading angle.

IV. CONCLUSION

Results from the Modified Three Gradient Method (MTGM), applied to a pulsed high intensity electron source, are presented. The method, experimental set-up, and experimental results referring to the non-destructive beam emittance measurements are presented. The MTGM makes possible the non-destructive determination of beam emittance in a space charge presence. The method is based on an integration of both beam cross-section measurements, realized in the three-gradient arrangement, and the beam envelope equation for an axially symmetric configuration. The experimental data is processed with a numerical matching program to determine the emittance and diameter. In the program, the σ matrix method was used to find the least square fitting to the measured cross-over curve to find the emittance; the envelope equation was solved with the numerical method of the 4^{th} order of the Runge-Kutta method to obtain beam radius. The measurement error is also analyzed. For the experimental beam, the normalized edge emittance is about 112 0π mm mrad.

ACKNOWLEDGMENTS

The authors would like to thank the members of the testing and operating team for their contribution to this work.

[1] Weiss M. The 1987 CERN Accelerator School, Aarhus, Denmark, 1986, 162–163.
[2] Ke J L, Zhou C G, Qiu R. High Power Laser Partic Beam, 2013, **8**: 2067–2070. (in Chinese)
[3] Dong J M and Wang S M. Nucl Tech, 2005, **28**: 435–437. (in Chinese)
[4] Bartch R R, Ekdahl C, Eylon S, *et al*. Beam emittance diagnostic for the DARHT second axis injector, the 28th IEEE International Conference on Plasma Science and the 13th IEEE International Pulsed Power Conference (PPPS2001), Las Vegas, USA, Jun. 17–22, 2001, 1689–1692.
[5] Bardy J, Bonnafond C, Devin A, *et al*. Status of AIRIX Alignment and High Current Electron Beam Diagnostics, the 5th European Particle Accelerator Conference (EPAC96), Sitges, Barcelona, Jun. 10–14, 1996, 1588–1590.
[6] Dai Z Y. Ph.D. Thesis, China Academy of Engineering Physics, 2003. (in Chinese)
[7] Guan Z. Calculated method. Beijing (CHN): Tsinghua University Press, 1996. (in Chinese)
[8] Chen S F. Time-resolved beam profile measurements of high-current, short–pulse electron beam. Report of Postdoctoral Work, China Academy of Engineering Physics, 2001. (in Chinese)
[9] Physics Manual Team. Physics manual. Fuzhou (CHN): Fujian People's Press, 1991, 825–827. (in Chinese)
[10] Li Q Y, Wang N C, Yi D Y. Numerical calculations. Wuhan (CHN): Huazhong Theory and Technology University Press, 1982, 97–105. (in Chinese)
[11] Zhang Z. Ph.D. Thesis, Peking University, 2010. (in Chinese)
[12] Lü J Q. Optics of charged particle beams. Beijing (CHN): Senior Education Publishing House, 2004, 1–78. (in Chinese)
[13] Zhang Z. Master Thesis, China Academy of Engineering Physics, 2004. (in Chinese)